Malaysian Journal of Medicine and Health Sciences Vol. 6 (2) June 2010: 71-92

Functional Specialisation and Effective Connectivity in Cerebral Motor Cortices: An fMRI Study on Seven Right Handed Female Subjects

[1]Ahmad Nazlim Yusoff*, [1]Mazlyfarina Mohamad, [1]Aini Ismafairus Abd Hamid, [2]Wan Ahmad Kamil Wan Abdullah, [1]Mohd Harith Hashim, & [3]Nurul Zafirah Zulkifli

[1]Functional Image Processing Laboratory (FIPL), Diagnostic Imaging & Radiotherapy Programme, Faculty of Allied Health Sciences, Universiti Kebangsaan Malaysia, Jalan Raja Muda Abdul Aziz, 50300 Kuala Lumpur

[2]Department of Radiology, School of Medical Sciences, Universiti Sains Malaysia, 16150 Kubang Kerian, Kelantan

[3]Department of Radiology, Sunway Medical Centre, No. 5 Jalan Lagoon Selatan, Bandar Sunway, 46150, Petaling Jaya, Selangor Darul Ehsan

ABSTRACT

Objective: This study investigates functional specialisation in, and effective connectivity between the precentral gyrus (PCG) and supplementary motor area (SMA) in seven right handed female subjects. **Methods:** Unimanual (UNI_{right} and UNI_{left}) and bimanual (BIM) self-paced tapping of hand fingers were performed by the subjects to activate PCG and SMA. Brain activations and effective connectivity were analysed using statistical parametric mapping (SPM), dynamic causal modeling (DCM) and Bayesian model selection (BMS) and were reported based on group fixed (FFX) and random (RFX) effects analyses. **Results:** Group results showed that the observed brain activation for UNI_{right} and UNI_{left} fulfill contralateral behavior of motor coordination with a larger activation area for UNI_{right}. The activation for BIM occurs in both hemispheres with BIM_{right} showing higher extent of activation as compared to BIM_{left}. Region of interest (ROI) analyses reveal that the number of activated voxel (NOV) and percentage of signal change (PSC) on average is higher in PCG than SMA for all tapping conditions. However, comparing between hemispheres for both UNI and BIM, higher PSC is observed in the right PCG and the left SMA. DCM and BMS results indicate that most subjects prefer PCG as the intrinsic input for UNI_{right} and UNI_{left}. The input was later found to be bi-directionally connected to SMA for UNI_{right}. The bi-directional model was then used for BIM in the left and right hemispheres. The model was in favour of six out of seven subjects. DCM results for BIM indicate the existence of interhemispheric connectivity between the right and left hemisphere PCG. **Conclusion:** The findings strongly support the existence of functional specialisation and integration i.e. effective connectivity in human brain during finger tapping and can be used as baselines in determining the probable motor coordination pathways and their connection strength in a population of subjects.

INTRODUCTION

The underlying objectives in modeling human brain function as proposed by Friston[1] rest mainly on the understanding of the relationships between the conceptual, anatomical, statistical and causal nature of the brain and the brain responses. These objectives pertaining to identifying specialised functional areas (the analyses of regionally specific effects: which area constitute a neuronal system) and determining the integrative function among specific areas (analyses of inter-regional effects: what are the interactions between the elements of a given neuronal system)[1]. The latter can then be divided into two specific objectives which are commonly referred to as functional connectivity (determination of the temporal correlation between spatially remote neurophysiological events) and effective connectivity (determination of the influence that the elements of a neuronal system exert over another)[1].

The most common imaging technique used in exploring the structure and function of human brain with regard to functional specialisation and integration is functional magnetic resonance imaging (fMRI)[2,3]. The ability of fMRI in detecting the effects of small metabolic changes in the brain lies in the state-of-the-art imaging technique or pulse sequence invented by Mansfield; the Echo Planar Imaging (EPI)[4,5] and the discovery of a remarkable endogenous contrast agent; the oxyhemoglobin[6-8]. The invention of EPI and the discovery of oxyhemoglobin as an endogenous contrast agent (Blood Oxygenation Level Dependent (BOLD), has since shed light on a vast number of studies in functional neuroimaging using fMRI.

*Corresponding author: *nazlim@fskb.ukm.my*

In a standard functional neuroimaging analysis of fMRI data, a statistical model is usually fit to the data by means of the general linear model (GLM). The model explains the data in terms of a linear combination of the explanatory variables plus an error term (ε). The model in matrix notation can be written as $Y = X\beta + \varepsilon$ where Y is the column vector of observations, ε is the column vector of error terms and β is the column vector of parameters. The model parameters are then estimated by means of the least square fitting method. Once the model is fitted, one then has to look for any effect such as the difference between active and rest states. To achieve this, an independent *t*-test is conducted on each brain voxel that tests for the effect of interest, resulting in a large volume of statistic for the whole brain volume. The effect size or the difference between active and rest states and the *t* values obtained are then compared to that of the null distribution for the *t* statistic. Finally, a decision has to be made whether this volume of statistic shows any evidence of the effect in which is studied. In other words, for a given voxel, the general linear model, by means of the least square fitting method, will figure out just what type that voxel is by modelling it as a linear combination of the hypothetical time series. The fitting or estimation entails finding the parameter values such that the linear combination best fits the measured data. The same general linear model can be used for all voxels but with different set of parameters for each voxel.

This study is a continuation of our previous work on a single subject[9]. In this study, the brain functional organisation i.e. functional specialisation and integration were investigated on multiple subjects with regards to the activation in the cerebral motor cortices evoked by finger tapping. It has been established that the primary motor area (M1) in the precentral gyrus (PCG) and the supplementary motor area (SMA) are involved in movement preparation and execution of motor action[10]. Establishing a reliable model of how these areas interact is crucial for a better understanding of the mechanism underlying motor function in both healthy subjects and patients[11]. Such decisions are of great practical relevence since we still lack detailed knowledge about the anatomical connectivity of the human brain[12]. In this study, group analyses were conducted by means of fixed (FFX) and random (RFX) effects analyses and inferences based on the group responses were made onto the whole subject. A conjunction analysis was then performed to search for common activated areas among the subjects. The connectivity measure between regions of interest were further studied and evaluated by implementing the dynamic causal modeling (DCM)[13] to model interactions among neuronal populations at cortical level.

A fundamental limitation of this study is that the results obtained are not suitable to be inferred to the whole population of right handed female subjects but are valid as long as the subjects under study are concerned. It has been suggested[14] that to achieve 80% power at the single voxel level for typical activations, thresholded at significant level (α) = 0.05, an fMRI study needs to have at least 12 subjects for an inference to be valid over a population of subjects.

MATERIALS AND METHODS

Subject

Functional magnetic resonance imaging (fMRI) examinations were performed on seven right-handed healthy female subjects. The average age and standard deviation is 23.6 ± 1.7 years old. Two of the subjects were Chinese while the rest were Malays. The subjects were given informed consent and screening forms as required by the Research and Medical Research Ethics Committee of the Universiti Kebangsaan Malaysia (UKM). The subjects were interviewed on their health condition prior to the scanning session and were confirmed to be healthy. Prior to the fMRI scans, the subjects' handedness were tested using the Edinburgh handedness inventory. All the subjects were confirmed to be right-handed. The subjects were also told not to move their head during the scan. Immobilizing devices were used together with the head coil in order to minimise head movement. Demographical data for all the subjects are depicted in Table 1.

Table 1 Demographical data for all subjects

Subject	Gender	Age	Race	Handedness
S1	Female	22	M	Right
S2	Female	25	C	Right
S3	Female	25	M	Right
S4	Female	26	M	Right
S5	Female	22	M	Right
S6	Female	22	M	Right
S7	Female	23	C	Right

M: Malay; C: Chinese

fMRI Scans

Functional magnetic resonance imaging (fMRI) scans were conducted in the Department of Radiology, Universiti Kebangsaan Malaysia Hospital. Functional images were acquired using a 1.5 tesla magnetic resonance imaging (MRI) system (Siemens Magnetom Vision VB33G) equipped with functional imaging option, echo planar imaging (EPI) capabilities and a radiofrequency (RF) head coil used for signal transmission and reception. Gradient Echo - Echo Planar Imaging (GRE-EPI) pulse sequence with the following parameters were applied : repetition time (TR) = 5 s, acquisition time (TA) = 3 s, echo time (TE) = 66 ms, field of view (FOV) = 210 × 210 mm, flip angle = 90°, matrix size = 128 × 128 and slice thickness = 4 mm. Using the midsagittal scout image (TR = 15 ms, TE = 6 ms, FOV = 300 × 300 mm, flip angle = 30 , matrix size = 128 × 128 and magnetic field gradient = 15 mT/m) produced earlier, 35 axial slice positions (1 mm interslice gap) were oriented in the anterior-posterior commissure (AC-PC) plane. This covers the whole brain volume. In addition, high resolution anatomical images of the entire brain were obtained using a strongly T1-weighted spin echo pulse sequence with the following parameters : TR = 1000 ms, TE = 30 ms, FOV = 210 × 210 mm, flip angle = 90 , matrix size = 128 × 128 and slice thickness = 4 mm.

Experimental paradigm

The subjects were instructed on how to perform the motor activation task and were allowed to practice prior to the scanning. The subjects had to press all four fingers against the thumb beginning with the thumb-index finger contact and proceeding to the other fingers in sequence and then begin anew with contact between thumb and index finger again. This study used a self-paced finger movement. The tapping of the fingers would approximately be twice in one second (using an intermediate force between too soft and too hard). A six-cycle active-rest paradigm which was alternately cued between active and rest was used with each cycle consisting of 10 series of measurements during active state and 10 series of mesurements during resting state. The tapping of the fingers were done unimanually (UNI_{left} or UNI_{right}) or bimanually (BIM) in alternate fashion as can be seen in Figure 1(a). Each functional measurement produces 20 axial slices in 3 s (one image slice in 150 ms) with an inter-measurement interval of 2 s. The measurement started with active state. The imaging time for the whole functional scans is 600 s (10 minutes) which produces 120 × 20 = 2400 images in total. A high resolution T2*-weighted images were obtained using the voxel size of 1.64 mm × 1.64 mm × 4.00 mm.

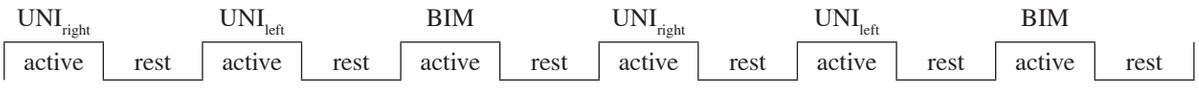

(a)

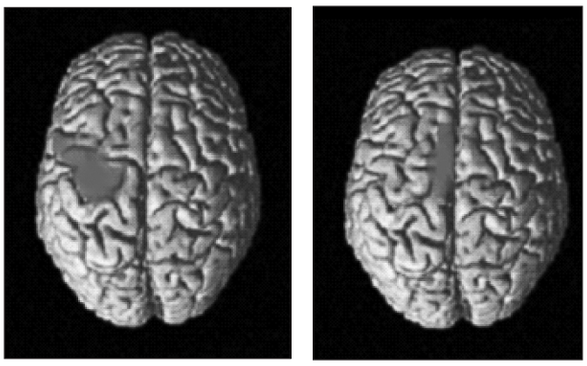

PCG SMA

(b)

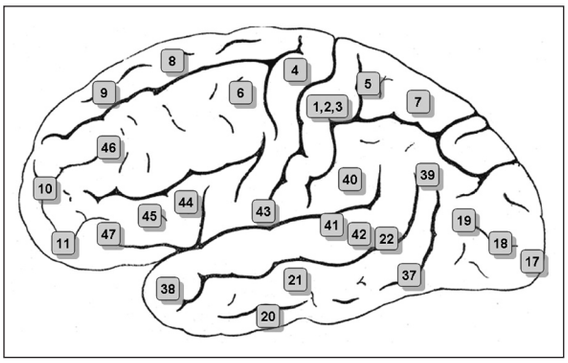

(c)

Figure 1 (a) The active-rest block paradigm used in this study, (b) the 3-D diagram of a brain showing the location of precentral gyrus (PCG) and supplementary motor area (SMA) in the left hemisphere and c) the Brodmann areas of a human brain (*Source*: Wikipedia, The Free Encyclopedia)

Post processing of the fMRI data

All the functional (T2*-weighted) and structural (T1-weighted) images were sent to Universiti Kebangsaan Malaysia Hospital (HUKM) MedWeb and were later retrieved in the Functional Image Processing Laboratory (FIPL), Diagnostic Imaging & Radiotherapy Programme, Faculty of Allied Health Sciences, UKM Kuala Lumpur for further

analyses. Image analyses were performed using a personal computer (PC) with a high processing speed and large data storage. The MATLAB 7.4 – R2007a (Mathworks Inc., Natick, MA, USA) and Statistical Parametric Mapping (SPM5) (Functional Imaging Laboratory, Wellcome Department of Imaging Neuroscience, Institute of Neurology, University College of London) software packages were used for that purposes. The raw data in DICOM (.dcm) format were transformed into Analyze (.hdr, .img) format by means of SPM5. Functional images in each measurement were realigned using the 6-parameter affine transformation in translational (*x, y* and *z*) and rotational (pitch, roll and yaw) directions to reduce artifacts from subject movement and in order to make intra and inter subject comparison in a meaningful way[15]. In the process, a reference image (the first image of a measurement serie) is chosen which remains stationary in space. The other images (source images) are then spatially transformed to match the reference image. A mapping is determined from each voxel position in the reference to a corresponding position in the source image. The source images are then resampled at the estimated position[16].

After realigning the data, a mean image of the series is used to estimate some warping parameters that map it onto a template that already conforms to a standard anatomical space (EPI template provided by the Montreal Neurological Institute - MNI)[15]. The complexity and variability of the human brain across subjects is so great that reliance on maps and atlases (such as construction of averages, templates and models) is essential to manipulate, analyse and interpret brain data effectively[17]. The normalisation procedure used a 12-parameter affine transformation where the parameters constitute a spatial transformation matrix[16]. The images were then smoothed using a 6-mm full-width-at-half-maximum (FWHM) Gaussian kernel. Activated voxels were identified by the general linear model approach by estimating the parameters of the model and by deriving the appropriate test statistic (*T* statistic) at every voxel. Statistical inferences were finally obtained on the basis of SPM and the Gaussian random field theory[15]. The inferences were made using the *T*-statistic at corrected ($\alpha_{FWE} = 0.05$) and uncorrected ($\alpha = 0.001$) significant levels for group FFX and RFX respectively. For the analysis of conjunction, the significant level is taken at $\alpha = 0.1$. Steps taken in data analyses using SPM have been completely described in various similar studies[9,18-21].

Region of interest analyses

The region of interest (ROI) analyses were performed in order to compare the response of the brain due to lateralisation (left and right) and task (UNI_{right}, UNI_{left} and BIM). The ROIs were the activation clusters obtained from the subjects' activation map which were defined using the softwares automated anatomical labelling (AAL)[22] at $\alpha_{FWE} = 0.05$ and WFU Pick Atlas[23] at $\alpha = 0.1$. The two selected ROIs were bilateral precentral gyrus (PCG) and supplementary motor area (SMA). These regions are chosen to be the same to those used in DCM analyses, which will be explained below. Small volume correction was performed within the predefined ROIs[24]. The percentage of signal change (PSC) relative to the baseline was extracted from the ROIs using MarsBar toolbox for SPM[25].

Dynamic causal modeling (DCM)

The dynamic causal modeling (DCM) was applied in evaluating the effective connectivity[13] between the two selected brain regions in and between the right and left hemispheres. The two cortical brain regions which have been found to be involved in motor processing are the primary motor area (M1) in the precentral gyrus (PCG) and supplementary motor area (SMA). The pre-motor cortex (PMC) was not included in the present DCM analyses due to the inconsistency of the activation in the respective pre-motor area even at a lower significance level. This could be due to the nature of the task done by the subjects that did not involve the integration of sensory information, which is one of functions of PMC. Figure 1(b) indicates the location of the two regions in the left hemisphere. These two regions of interest (ROIs) were found to be activated in all participating subjects but the coordinates of the activation peaks differ by a few millimeters from subject to subject. The peak coordinates of the ROIs on the statistical parametric maps (SPMs) produced by RFX were taken as the anatomical landmark and the corresponding anatomical structures were confirmed by superimposing the SPMs onto the coplanar high resolution T1-weighted images using the Anatomy Toolbox[26] and by using the WFU Pick Atlas software[23]. The anatomical constraints are; 1) the M1 coordinates had to be in the PCG and 2) the SMA coordinates had to be in the dorsal medial wall within the interhemispheric fissure. A spherical volume of 4 mm in radius was extracted from the ROIs from which the effective connectivity between the ROIs was calculated via DCM. This approach has been found to be successful in measuring the effective connectivity between motor associated areas[11].

Three levels of DCM analyses were used in this study. In the first level, the input centre for UNI_{right} and UNI_{left} is determined by means of model comparison using Bayesian inferences. Two models, Models 1 and 2 were initially constructed to represent the most probable direction and strength of the motor input with the signal initially generated in PCG or in SMA, see Figure 2. For Model 1, the signal is said to traverse from PCG to SMA and from SMA to PCG with PCG as the input. In Model 2, the signal is sent from SMA to PCG and back to SMA with the SMA as the input.

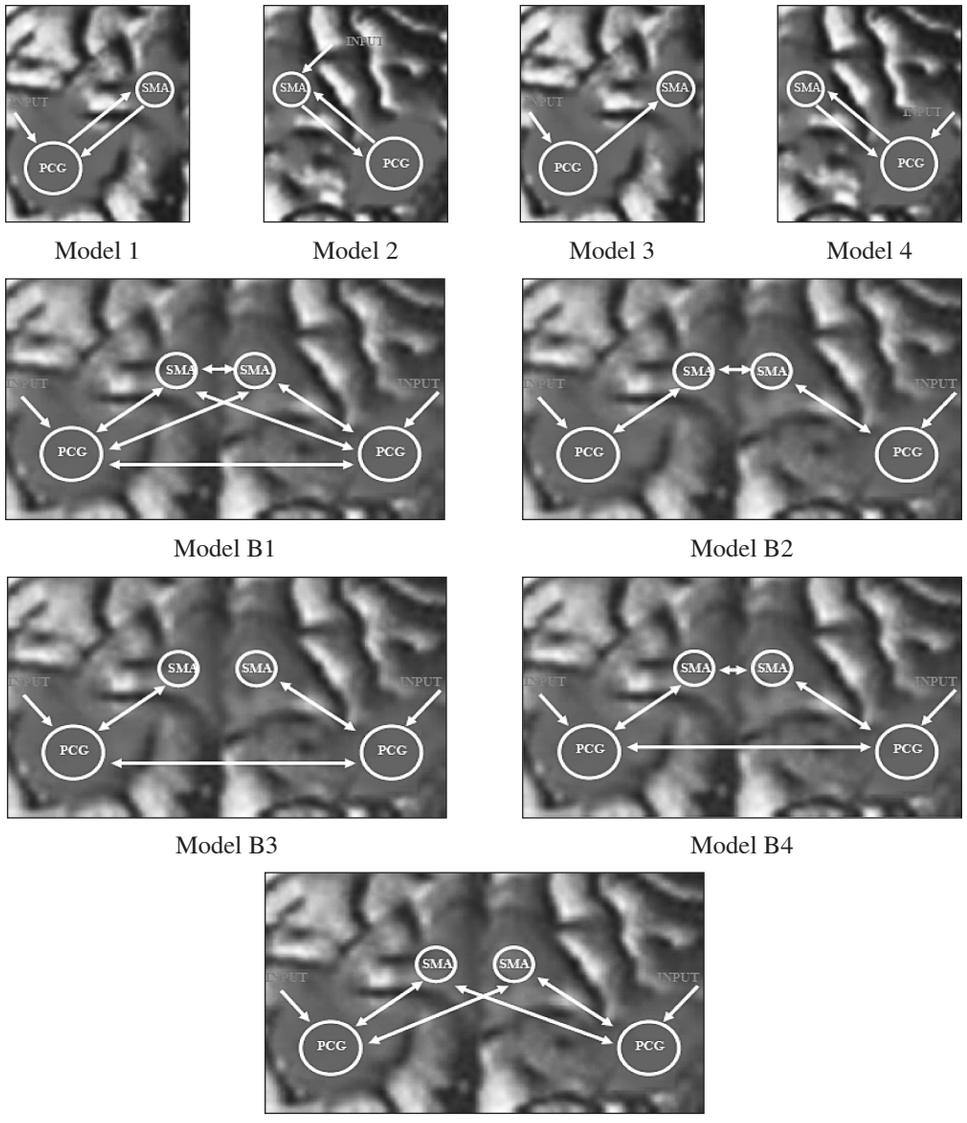

Figure 2 Model 1 and 2 are used in determining the input center for UNI. Model 3 and 4 are used to model the unimanual (UNI) type of finger tapping with precentral gyrus (PCG) as the input center. Model 5 (or B1) is the full connectivity model for bimanual (BIM) and Model B2 – B5 are the reduced models of B1. (→) represent the input while (↔) represent forward and backward connections between any two areas

The two models are then estimated in order to determine the input strength and its posterior probability and to determine the connection and the probability of the existence of the connection by means of Bayesian estimation procedures encapsulated in DCM. Model comparisons are made based on Akaike Information Criterion (AIC) and Bayesian Information Criterion (BIC)[12] to determine the winning model. Empirically, AIC is observed to be biased towards complex models and BIC towards simple model. For a model to be accepted as the most probable model, a good agreement between AIC and BIC must be achieved. This means, the probability of getting a correct model (m) given the data (y), or $p(y|m)$, is high in both AIC and BIC frameworks.

The model with the most probable input center obtained from the first level is entered into the second level. In this level, the two uni-direction and bi-direction models as shown respectively by Model 3 and Model 4, i.e. with PCG as the input, are tested onto all subjects to determine which model would be the most suitable to represent the connectivity during UNI_{right} and UNI_{left} for all the subjects under study. The models are again estimated and compared in a Bayesian framework as mentioned above to obtain the winning model. The most probable model obtained in the second level is then used in DCM analyses of BIM in the third level. The same model is assumed for both BIM_{right}

and BIM_{left} with the inclusion of interhemispheric connections between $SMA_{right} \leftrightarrow SMA_{left}$, $PCG_{right} \leftrightarrow PCG_{left}$, $SMA_{right} \leftrightarrow PCG_{left}$ and $PCG_{right} \leftrightarrow SMA_{left}$. Model 5 is the full connectivity model for BIM. From Model 5 (named as B1 in the third level analysis), four reduced models (Model B2 – B5) were constructed and entered into DCM to determine the most probable model for BIM type of self-paced finger tapping. See Figure 2 for a complete set of models discussed above.

RESULTS

Brain activation during UNI_{right}, UNI_{left} and BIM: functional specialisation

Figures 3(a - d) shows the glass images or statistical parametric maps (SPMs) of the brain in neurological appearance (the left side of the image is the actual left side of the brain) representing the results obtained from statistical inference made on a single subject using fixed effects analysis (FFX), for UNI_{right}, UNI_{left} and BIM. Only the results for Subject 3, 5, 6 and 7 are shown. The SPMs were generated via the statistical parametric mapping (SPM5) analysis on each voxel using the *T*-contrast or SPM{T}. The results were projected onto the Tailairach-MNI stereotactic coordinates[27, 28]. The (<) symbols indicate the point of maximum intensity (global maximum) in the respective analysis with the coordinates shown on the left-hand side of the figures. The darker the voxel, the higher the intensity of the BOLD signal. The shadowed regions or blobs on the SPMs (shown in Figures 3(a - d)), hence, represent the statistical image of the effects of interest, for example the activated brain areas during finger tapping (right, left or bimanual). The results are obtained by taking the *p* value for each voxel smaller than a corrected alpha ($\alpha_{FWE} = 0.05$) value as significant, after correcting for multiple comparison.

(a) Subject 3

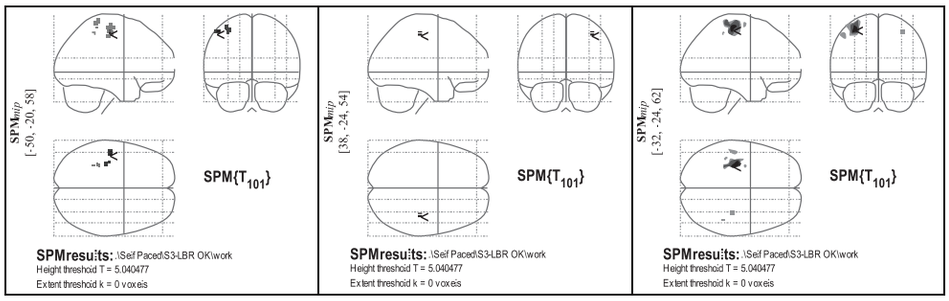

(b) Subject 5

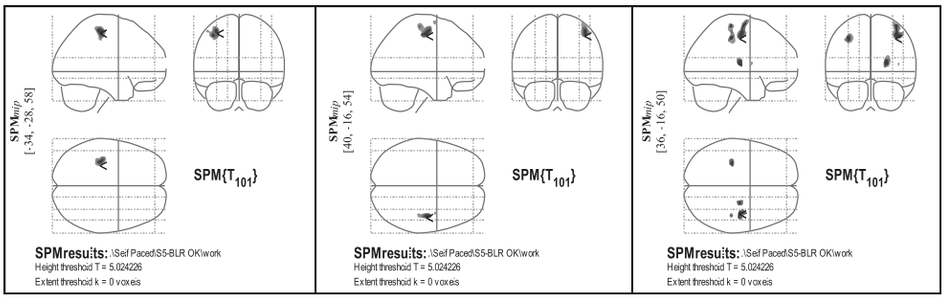

(c) Subject 6

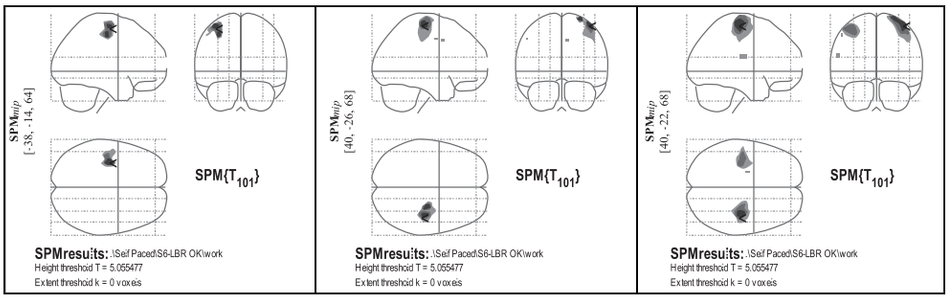

(d) Subject 7

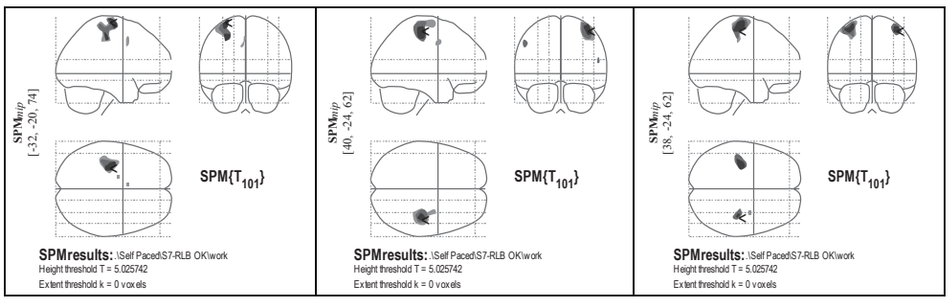

Figure 3 The statistical parametric maps (SPMs) obtained from a) Subject 3, b) Subject 5, c) Subject 6 and d) Subject 7 showing differences in spatial and height extent of brain activations due to unimanual (UNI_{right} and UNI_{left}) and bimanual (BIM) (in the order from left to right)

Figures 4(a) shows the glass images or the statistical parametric maps (SPMs) of the brain representing the average results obtained from statistical inference made on all subjects by means of fixed effects analysis (FFX), for UNI_{right}, UNI_{left} and BIM, while Figure 4(b) are the results derived from random effects analysis (RFX).

(a)

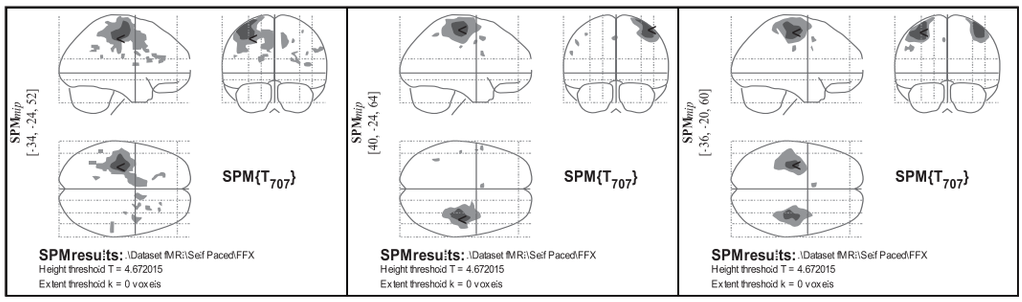

(b)

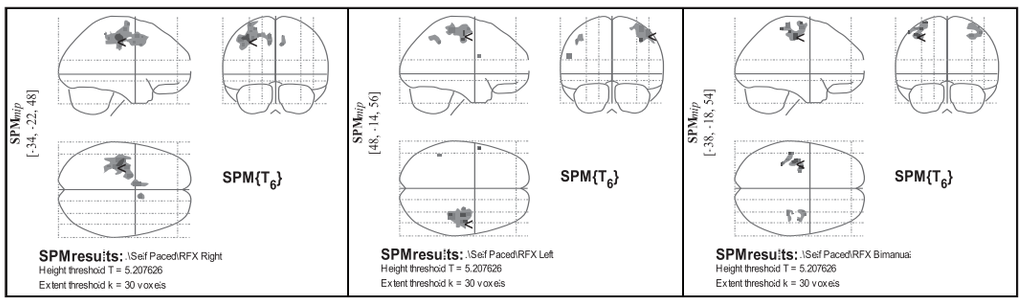

(c)

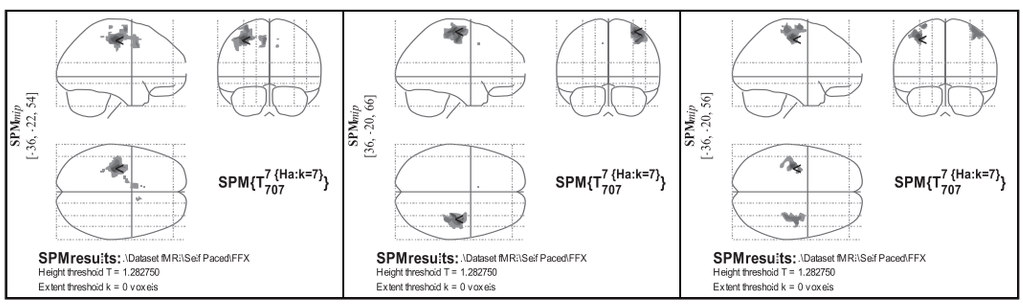

Figure 4 The statistical parametric maps (SPMs) obtained from a) fixed effects (FFX), b) random effects (RFX) and c) conjunction analyses for all subjects showing brain activations due to unimanual (UNI_{right} and UNI_{left}) and bimanual (BIM) (in the order from left to right)

Table 2 shows some statistical data, MNI coordinates at the point of maximum intensity in each respective cluster and the anatomical areas in which the maximum in the brain activation due to UNI_{right}, UNI_{left} and BIM occurred. The data were obtained from the SPMs of FFX shown in Figure 4(a). The activated areas are anatomically interpreted using a MATLAB based SPM5 Anatomy toolbox, which enables the integration of the probabilistic cytoarchitectonic maps with the results generated by SPM[26].

Table 2 Statistical data, Tailarach-MNI coordinates (*x, y, z*) and the respective anatomical areas obtained from unimanual (UNI_{right} and UNI_{left}) and bimanual (BIM) by means of fixed-effects analysis (FFX). Only the details of the anatomical areas of the main cluster are tabulated

Set-level		Cluster-level			Voxel-level					
Movement	$p_{corrected}$	Clusters	$p_{corrected}$	No. of activated voxel	$p_{corrected}$	*t*-value	*x, y, z* (mm)			Anatomical area
UNI_{right}	< 0.001	16	< 0.001	3157	< 0.001	13.31	-34	-24	52	Left postcentral gyrus, assigned to BA4p, probability 50% (30 – 50%)
					< 0.001	12.55	-35	-16	58	Left precentral gyrus, assigned to BA6, probability 60% (60 – 100%)
					< 0.001	10.27	-48	-20	56	Left postcentral gyrus, assigned to BA1, probability 90% (70 – 90%)
UNI_{left}	< 0.001	6	< 0.001	2270	< 0.001	16.45	40	-24	64	Right precentral gyrus, assigned to BA6, probability 70% (50 – 80%)
					< 0.001	10.54	34	-6	70	Right superior frontal gyrus
					0.001	5.61	20	-6	78	Not found in any probability map
BIM_{right}	< 0.001	6	< 0.001	1917	< 0.001	13.51	-36	-20	60	Left precentral gyrus, assigned to BA6, probability 70% (20 – 100%)
					< 0.001	8.96	-42	-32	64	Left postcentral gyrus, assigned to BA1, probability 90% (0 – 90%)
					< 0.001	6.19	-32	-38	70	Left postcentral gyrus, assigned to BA1, probability 50% (50 – 70%)
BIM_{left}			< 0.001	1783	< 0.001	13.17	38	-26	66	Right precentral gyrus, assigned to BA6, probability 80% (60 – 90%)
					< 0.001	11.22	40	-14	60	Right precentral gyrus, assigned to BA6, probability 70% (60 – 90%)
					< 0.001	9.68	34	-8	68	Right superior frontal gyrus, 10% probability for BA6 (0 – 10%)

There are 16 significant clusters for UNI_{right}. However, there exist only one main activation cluster for UNI_{right} which occurs in the left hemisphere. Contralaterality is fulfilled in which the motor coordination of the right hand fingers is controlled by motor cortices in the left hemisphere. A number of 3157 activated voxels ($t > 4.67$, $p_{FWE} < 0.05$) constituted the main cluster with six local maxima at the Talairach-MNI coordinates of (-34,-24,52), (-36,-16,58), (-48,-20,56), (-28,-16,74), (-8,4,50) and (-46,-22,36) which occurs in the left postcentral and precentral gyrii and left supplementary motor area (SMA), see Table 2. It is found that 35.3% of cluster is in the left BA6 (25.3% activated), 8.2% of cluster in the left BA2 (24.6% activated), 8.2% of cluster in the left BA4p (44.5% activated) and 7.9% of cluster in the right BA3b (33.7% activated), see Figure 1(c) for the definition of Brodmann areas (BA) of a human brain.

For UNI_{left}, there are 6 significant activation clusters that survive the height threshold of $\alpha_{FWE} = 0.05$. The main cluster consists of 2270 activated voxels ($t > 4.67$). The main cluster has three maxima at the Talairach-MNI coordinates of (40,-24,64), (34,-6,70) and (20,-6,78) which occur in the right precentral and superior frontal gyrii. The cluster covered 36.2% of the right BA6 (18.8% activated), 15.2% of the right BA1 (40.5% activated), 9.0% of the right BA3b (20.8% activated) and 7.4% of the right BA2 (15.2% activated). Contralaterality is also fulfilled for UNI_{left}.

For BIM, there are also 6 significant activation clusters from which two are considered as the main clusters, evoked by the simultaneous tapping of the right and left hand fingers, denoted by BIM_{right} and BIM_{left} respectively. The activation due to BIM_{right} occurs in the left pre and postcentral gyrii with three maxima at Talairach-MNI coordinates of (-36,-20,60), (-42,-32,64) and (-32,-38,70). The total number of activated voxel is 1917 ($t > 4.67$, $p_{FWE} < 0.05$) with

38.9% of the cluster is in the left BA6 (17.0% activated), 17.0% is in the left BA1 (32.0% activated), 10.0% is in the left BA4p (33.0% activated) and 9.5% is in the left BA4a (14.0% activated). On the other side of the brain hemisphere, BIM_{left} activates a number of 1783 voxels ($t > 4.67$, $p_{FWE} < 0.05$) in the right precentral, superior frontal and postcentral gyrii with 4 maxima at Talairach-MNI coordinates of (38,-26,66), (40,-14,60), (34,-8,68) and (36,-44,62). It was found that 41.2% of cluster is in the right BA6 (16.8% activated), 15.0% of cluster is in the right BA1 (31.4% activated), 8.8% of cluster is in the right BA3b (13.0% activated) and 8.0% of cluster is in the right BA3b (14.6% activated).

RFX gives similar results as FFX, as shown in Figure 4(b) and Table 3. For UNI_{right}, three significant clusters survive a height threshold of $\alpha = 0.001$ and a spatial threshold of 30 voxels (clusters with a number of activated voxels of less than 31 are eliminated). There are a total of 818 activated voxels ($t > 5.21$) in the main cluster which covers parts of the left post and precentral gyrii with 5 maxima which are at Talairach-MNI coordinates of (-34,-22,48), (-40,-18,52), (-42,-16,50), (-42,-18,42) and (-24,-20,54). The results indicate that 27.8% of the main cluster is in the left BA6 (5.2% activated), 21.5% of cluster is in the left BA4p (30.3% activated), 13.9% of cluster is in the left BA3b (15.4% activated) and 9.8% of cluster is in the left BA2 (7.6% activated).

Table 3 Statistical data, Tailarach-MNI coordinates (*x, y, z*) and the respective anatomical areas obtained from unimanual (UNI_{right} and UNI_{left}) and bimanual (BIM) by means of random-effects analysis (RFX). Only details of the anatomical areas of the main cluster are tabulated. The data were obtained after thresholding the statistical parametric maps (SPMs) at $\alpha = 0.001$ and allowing only clusters with number of activated voxel (NOV) of more than 30

Set-level		Cluster-level			Voxel-level		*x, y, z* (mm)			Anatomical area
Movement	$p_{uncorrected}$	Clusters	$p_{uncorrected}$	No. of activated voxel	$p_{uncorrected}$	*t*-value				
UNI_{right}	< 0.001	3	< 0.001	818	< 0.001	15.89	-34	-22	48	Left postcentral gyrus, assigned to BA4p, probability 70% (40 – 80%)
					< 0.001	14.65	-40	-18	52	Left precentral gyrus, assigned to BA4a, probability 50% (40 – 60%)
					< 0.001	11.27	-42	-18	42	Left postcentral gyrus, assigned to BA4p, probability 60% (56 – 60%)
UNI_{left}	< 0.001	3	< 0.001	663	< 0.001	17.85	48	-14	56	Right precentral gyrus, assigned to BA6, probability 60% (50 – 80%)
						16.87	38	-16	46	Right precentral gyrus, assigned to BA4a, probability 50% (40 – 70%)
						11.93	38	-34	60	Right postcentral gyrus, assigned to BA1, probability 80% (40 – 80%)
BIM_{right}	< 0.001	6	< 0.001	124	< 0.001	11.48	-38	-18	54	Left precentral gyrus, assigned to BA4a, probability 50% (30 – 60%)
			< 0.001	90	< 0.001	10.61	-50	-26	58	Left postcentral gyrus, assigned to BA1, probability 90% (90 – 90%)
					< 0.001	10.21	-32	-38	64	Left postcentral gyrus, assigned to BA2, probability 50% (40 – 70%)
					< 0.001	6.42	-44	-28	64	Left postcentral gyrus, assigned to BA1, probability 70% (60 – 100%)
			< 0.001	50	< 0.001	10.13	-28	-12	72	Left precentral gyrus, assigned to BA6, probability 60% (0 – 70%)
BIM_{left}			< 0.001	113	< 0.001	8.20	32	-10	64	Right superior frontal gyrus, 20% probability for BA6 (10 – 50%)
					< 0.001	7.63	46	-14	58	Right precentral gyrus, assigned to BA6, probability 90% (60 – 100%)
					0.001	5.51	32	-4	70	Right superior frontal gyrus
			< 0.001	49	< 0.001	7.40	38	-30	68	Right postcentral gyrus, assigned to BA6, probability 60% (0 – 50%)
			0.002	31	< 0.001	6.63	30	-30	52	Right postcentral gyrus, assigned to BA4p, probability 40% (10 – 40%)

For UNI_{left}, 3 significant clusters survive the height threshold of $\alpha = 0.001$ and spatial threshold of 30 voxels. Two of the clusters are in the left inferior parietal lobe and left precentral gyrus in the left hemisphere. The main activation cluster consist of 5 maxima, 3 of which are shown in Table 3. Their Talairach-MNI coordinates are (48,-14,56), (38,-16,46) and (38,-34,60). A number of 663 voxels are activated ($t > 5.21$); 34.5% of cluster is in the right BA6 (5.2% activated), 23.1% of cluster is in the right BA1 (17.9% activated), 16.5% of cluster is in the BA4a (9.1% activated) and 9.0% of cluster is in the right BA3b (6.1% activated).

Six significant activation clusters are observed in both the right and left hemispheres for BIM (BIM_{right} and BIM_{left}) at significant level of $\alpha = 0.001$ and spatial threshold of 30 voxels ($t > 5.21$). The areas involved are the precentral, postcentral and superior frontal gyrii. For the main left hemisphere cluster (124 voxels centered at (-38,-18,54)), 34.1% of the cluster is in the left BA4a (3.2% activated), 34.0% of cluster is in the left BA4p (7.2% activated), 17.8% of cluster is in BA6 (0.5% activated) and 13.3% of cluster is in BA3b (2.2% activated). For the 90-voxel cluster (centered at (-50,-26,58)), 77.4% of cluster is in the left BA1 (6.9% activated), 19.0% of cluster is in BA2 (1.6% activated), 2.2% of cluster is in BA4a (0.2% activated and 1.0% of cluster is in BA3b (0.1% activated). Finally, 80% of the 50-voxel cluster (centered at (-28,-12,72) is in BA6 (1.0% activated).

For the activation in the right hemisphere, the main cluster with 113 activated voxels and maximum activation at (32,-10,64) covers 58.3% of BA6 (1.5% activated), 1.4% of BA4a (0.1% activated), 0.4% of BA3b (0.1% activated) and 0.3% of BA1 (0.0% activated). For the second cluster centered at (38,-30,68) with 49 voxels activated, 52% of cluster is in BA6 (0.6% activated), 15.8% of cluster is in BA4a (0.6% activated) and 13.5% of cluster is in BA1 (0.8% activated). The third activation cluster with 31 activated voxel, centered at (30,-30,52). 66.1% of cluster is in BA4p (4.4% activated), 28.6% of cluster is in BA4a (0.7% activated) and 5.2% of cluster is in BA6 (0.0% activated). It can be concluded that the RFX results are in a good agreement with that obtained from FFX despite different significant levels used in both analyses.

The results obtained from the analyses of conjunction[15] on the present UNI_{right}, UNI_{left} and BIM datasets indicate that all subjects show common activation areas in the primary, secondary and associated motor areas, see Figure 4(c) and Table 4. However, the SPM results generated at significant level of $\alpha = 0.1$ indicate significant activation only at voxel level. Both the set and cluster level inferences about the activation clusters revealed insignificant brain activation. For UNI_{right}, 10 clusters of activation were detected in the left postcentral gyrus, precentral gyrus, supplementary motor area and middle cingulated cortex, as well as in the right supplementary motor area and middle cingulated cortex. The main cluster which has 474 activated voxels ($t > 2.30$) with the point of maximum activation at (-36,-22,54), shows that 30.6% of cluster is in the left BA4p (25.0% activated), 29.3% of cluster in the left BA6 (3.2% activated), 13.3% of cluster in the left BA4a (4.8% activated) and 13.2% of cluster is in the left BA3b (8.5% activated).

For UNI_{left}, the analysis of conjunction at significant level of $\alpha = 0.1$, reveals 2 clusters of activation which are in the right precentral gyrus and the left supplementary motor area. The main cluster in the right precentral gyrus consists of 684 activated voxels ($t > 2.9$) and has 6 maxima at (36,-20,66), (42,-16,58), (42,-18,52), (40,-10,64), (34,-22,6) and (46,-16,54). 47.0% of the cluster is in the right BA6 (7.0% activated), 15.8% is in the right BA1 (12.0% activated), 12.2% of cluster is in the right BA4a (6.5% activated) and 9.8% of cluster is in the right BA3b (6.5% activated). The secondary cluster which is in the left supplementary area consist of only one significant voxel at coordinates of (-6,10,46). It is very interesting to see that the analysis of conjunction for UNI_{right} and UNI_{left} has also reveals activated areas in the opposite hemisphere to the contralateral hemisphere i.e. the ipsilateral supplementary motor area and middle cingulated cortex. This clearly indicates the involvement of the ipsilateral side of human brain during unimanual tapping of fingers.

For BIM, 4 clusters of activation is revealed under a significant level of $\alpha = 0.1$, occurring in the precentral gyrus, postcentral gyrus and superior frontal gyrus. For BIM_{right}, the main cluster has 4 maxima in the left post and precentral gyrii which are centered at Talairach-MNI coordinates of (-36,-20,56), (-42,-32,64), (-46,-28,62) and (-38,-36,62) respectively. The main cluster has 200 activated voxel ($t > 1.5$) from which 28.1% of the main cluster is in the left BA1 (5.5% activated), 24.5% is in the left BA4p (8.4% activated), 21.1% of cluster is in the left BA4a (3.2% activated) and 19.8% of cluster is in the left BA6 (0.9% activated). The secondary cluster which is also located in the precentral gyrus, has only one maximum centered at Talairach-MNI coordinates of (-30,-12,70). 79.8% of this cluster is in the left BA6 (0.6% activated). For BIM_{left}, the main cluster has 6 maxima, all located in the right precentral gyrus. A number of 258 voxel are activated ($t > 1.5$) with 65.7% of cluster is in the right BA6 (3.9% activated), 8.6% is in the right BA4a (1.8% activated), 3.1% is in the right BA1 (0.9% activated) and 2.3% is in the right BA4p (1.3% activated). The secondary cluster for BIM_{left} occur at coordinates of (36,-2,66) in the right superior frontal gyrus. Only one voxel is activated.

Table 4 The statistics and anatomical area as revealed by conjunction analyses on all subjects. A relatively lower height threshold of $\alpha = 0.1$ (uncorrected) is used in obtaining the activation. No spatial threshold is used in conjunction analyses

Set-level			Cluster-level		Voxel-level					
Movement	$p_{corrected}$	Clusters	$p_{uncorrected}$	No. of activated voxel	$p_{uncorrected}$	*t*-value	x, y, z (mm)			Anatomical area
UNI_{right}	1.000	10	0.245	474	< 0.001	4.00	-36	-22	54	Left postcentral gyrus, assigned to BA4p, probability 40% (30 – 50%)
					0.002	2.82	-36	-14	56	Left precentral gyrus, assigned to BA6, probability 70% (60 – 80%)
					0.009	2.38	-45	-20	52	Left postcentral gyrus, assigned to BA1, probability 60% (20 -70%)
			0.672	71	0.026	1.94	-6	4	54	Left supplementary motor area, assigned to BA6, probability 60%, (60 – 80%)
					0.058	1.56	-10	4	42	Left middle cingulated cortex, 10% probability for BA6, (0 – 30%)
					0.068	1.48	-12	-2	56	Assigned to BA6, probability 40% (20 – 60%)
			0.905	9	0.027	1.93	10	6	42	Right middle cingulated cortex, 20% probability for BA6, (10 – 30%)
			0.926	6	0.067	1.48	-36	-30	68	Left postcentral gyrus, assigned to BA4a, probability 60% (0 – 60%)
			0.964	2	0.068	1.47	10	10	52	Right supplementary motor area, 30% probability for BA6 (20 – 30%)
			0.977	1	0.074	1.43	-18	-8	54	Not assigned, 20% probability for BA6 (0 – 40%)
			0.964	2	0.078	1.40	-30	-40	56	Left postcentral gyrus, assigned to BA2, probability 50% (20 – 70%)
			0.964	2	0.085	1.35	-20	-10	56	Assigned to BA6, probability 40% (20 – 70%)
			0.964	2	0.087	1.34	-8	12	46	Left supplementary motor area, 20% probability for BA6 (20 – 30%)
			0.977	1	0.089	1.32	-26	-12	58	Left precentral gyrus, assigned to BA6, probability 50% (30 – 50%)
UNI_{left}	1.000	2	0.177	648	< 0.001	3.43	36	-20	66	Right precentral gyrus, assigned to BA6, probability 100% (80 – 100%)
					0.001	3.13	42	-16	58	Right precentral gyrus, assigned to BA6, probability 80% (50 – 90%)
					0.001	3.10	40	-10	64	Right precentral gyrus, assigned to BA6, probability 50% (0 – 70%)
			0.977	1	0.070	1.46	-6	10	46	Left supplementary motor area, 20% probability for BA6 (20 – 30%)
BIM_{right}	1.000	4	0.453	200	< 0.001	3.69	-36	-20	56	Left precentral gyrus, assigned to BA4a, probability 60% (40 – 70%)
					0.036	1.79	-42	-32	64	Left postcentral gyrus, assigned to BA1, probability 90% (0 – 90%)
			0.784	34	0.012	2.25	-30	-12	66	Left precentral gyrus, assigned to BA6, probability 50% (0 – 60%)
BIM_{left}			0.391	258	0.003	2.78	38	-28	68	Right precentral gyrus, assigned to BA6, probability 70% (0 – 80%)
					0.005	2.59	42	-16	60	Right precentral gyrus, assigned to BA6, probability 80% (70 – 90%)
					0.023	2.00	38	-8	62	Right precentral gyrus, 30% probability for BA6 (0 – 50%)
				1	0.092	1.30	36	-2	66	Right superior frontal gyrus

Number of activated voxel (NOV) and percentage of signal change (PSC)

Table 5(a) shows the number of activated voxel (NOV) in PCG and SMA for all tapping conditions at uncorrected (α = 0.1 and 0.001) and corrected (α_{FWE} = 0.05) significance levels calculated from SPMs that are obtained from individual subjects, FFX and RFX. The data are obtained by means of WFU Pickatlas toolbox[23] which filtered out the activation in other areas, leaving only activation in the ROIs i.e. PCG and SMA.

Table 5(a) Number of activated voxel (NOV) at uncorrected 0.1, 0.001 and corrected 0.05 significance levels (α) calculated from SPMs that are obtained for all individual subjects, fixed-effects analysis (FFX) and random-effects analysis (RFX). The data shown are for the two regions of interest, namely the precentral gyrus (PCG) and supplementary motor area (SMA) and for all tapping conditions

		UNI_{right}		UNI_{left}		BIM_{right}		BIM_{left}	
	α	PCG	SMA	PCG	SMA	PCG	SMA	PCG	SMA
Subject 1	0.1	1798	636	1264	1059	1162	617	1063	988
	0.001	649	299	368	17	341	217	132	136
	0.05	292	194	143	2	166	120	46	58
Subject 2	0.1	1038	348	1327	192	1170	373	1040	341
	0.001	193	32	573	14	256	0	71	0
	0.05	76	1	391	7	73	0	0	0
Subject 3	0.1	1612	680	988	205	1510	759	1035	968
	0.001	664	70	278	18	751	56	178	70
	0.05	357	14	126	1	503	4	69	14
Subject 4	0.1	2107	743	1657	553	1730	530	1476	528
	0.001	1145	185	843	4	673	29	648	0
	0.05	859	119	565	0	421	7	378	0
Subject 5	0.1	1417	595	1399	333	1148	541	1833	624
	0.001	414	38	546	0	302	100	700	176
	0.05	190	9	386	0	115	31	432	71
Subject 6	0.1	2248	759	1835	475	1779	391	1652	712
	0.001	1159	55	977	45	1021	41	1088	93
	0.05	786	10	820	10	781	6	978	24
Subject 7	0.1	1827	763	1897	902	1586	927	1165	766
	0.001	822	164	826	15	697	123	437	96
	0.05	637	102	620	0	538	62	290	21
FFX	0.1	2511	1027	1907	868	1782	996	1781	1273
	0.001	1576	544	1267	171	1337	279	1183	100
	0.05	1377	435	1160	68	1188	154	1073	22
RFX	0.1	2147	853	1574	629	1547	655	1371	593
	0.001	292	116	384	7	111	25	114	0
	0.5	15	1	17	0	2	2	0	0

Table 5(b) The percentage of signal change (PSC) and its respective coordinates at the point of maximum intensity obtained from individual subject and fixed-effects analysis (FFX) for the two regions of interest, namely the precentral gyrus (PCG) and supplementary motor area (SMA), for all tapping conditions. The random-effects analysis (RFX) coordinates of the point of maximum intensity are shown for comparison

	UNI_{right}		UNI_{left}		BIM_{right}		BIM_{left}	
	PCG	SMA	PCG	SMA	PCG	SMA	PCG	SMA
Subject 1	0.362 -32,-22,48	0.313 -8,8,44	0.505 40,-28,68	0.226 10,8,74	0.586 -28,-10,66	0.345 -18,0,66	0.441 36,-28,70	0.453 10,4,68
Subject 2	0.599 -40,-18,70	0.196 -12,0,48	0.496 42,-20,62	0.219 2,-2,56	0.29 -38,-22,60	0.146 -2,-10,50	0.195 36,-18,52	0.139 6,-22,54
Subject 3	0.428 -34,-26,62	0.262 -10,2,46	0.469 38,-24,54	0.284 14,-6,48	0.547 -32,-24,62	0.293 -2,-4,50	0.444 36,-26,56	0.322 4,4,48
Subject 4	0.699 -36,-14,66	0.331 -8,4,50	0.39 36,-14,56	0.196 12,6,46	0.553 -34,-10,54	0.257 -8,6,52	0.524 38,-18,56	0.26 14,-14,54
Subject 5	0.52 -34,-28,58	0.299 -6,-16,58	0.562 40,-16,54	0.134 4,6,74	0.422 -34,-26,54	0.37 -12,-10,54	0.396 36,-16,50	0.395 14,-10,58
Subject 6	0.847 -38,-14,64	0.258 -6,6,44	1.577 40,-26,68	0.279 10,6,46	0.684 -34,-18,60	0.229 -4,0,46	1.794 40,-22,68	0.284 8,10,48
Subject 7	0.617 -32,-20,74	0.178 -4,6,50	-0.145 40,-24,62	0.296 6,2,54	0.03 -34,-22,62	0.253 -4,-2,58	0.439 38,-24,62	0.191 6,-6,62
FFX	0.331 -34,-20,52	0.203 -8,4,50	0.555 40,-24,64	0.109 8,2,54	0.366 -36,-20,60	0.115 -6,6,46	0.47 38,-26,66	0.101 8,8,46
RFX	- -40,-18,52	- -8,4,54	- 48,-14,56	- 10,2,54	- -38,-18,54	- -8,-2,64	- 34,-10,64	- 10,20,50

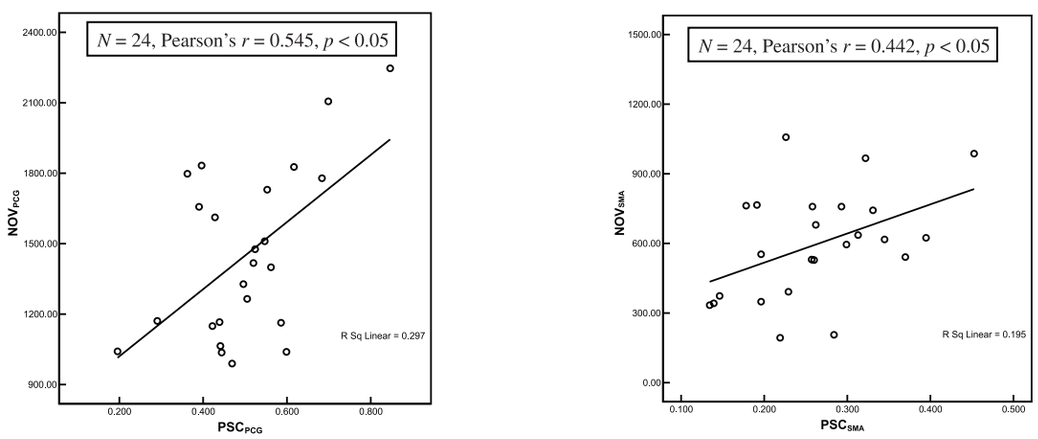

(a) (b)

Figure 5 Statistical packages for Social Sciences (SPSS) correlation results between the percentage of signal change (PSC) and number of activated voxel (NOV) measured in the two regions of interest (ROIs) namely precentral gyrus (PCG) and supplementary area (SMA)

The percentage of signal change (PSC) and its respective coordinates at the point of maximum intensity obtained from individual subject and FFX for the two regions of interest, namely the precentral gyrus (PCG) and supplementary

motor area (SMA), for all tapping conditions are tabulated in Table 5(b). The PSC values for RFX are not shown since it cannot be measured by means of RFX which uses the contrast of the parameter estimates in generating the SPMs. However, RFX coordinates of the point of maximum intensity are shown for comparison. The PSC values are measured using MarsBar toolbox for SPM[25].

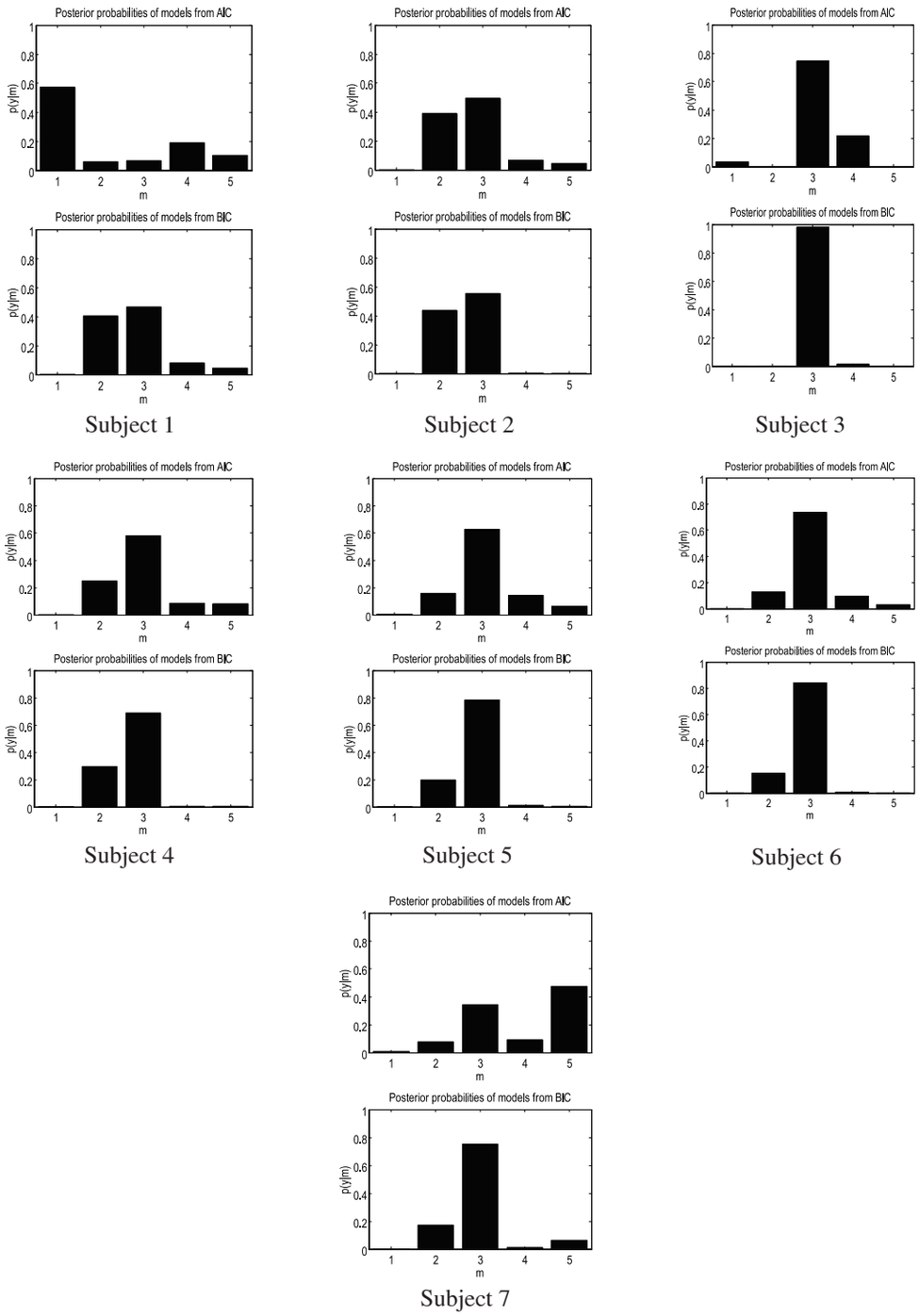

Figure 6 Results of Bayesian model selection (BMS) for bimanual (BIM) showing the agreement between Akaike Information Criterion (AIC) and Bayesian Information Criterion (BIC) on Model B3

Figure 5(a) and (b) show the results obtained from correlation analyses using Statistical Packages for Social Sciences (SPSS) software, between the two variables that are measured from the two ROIs as stated above. The purpose was to determine the existence of association between the two variables as well as its strength, direction and significance of

association. The data were taken from the two ROIs from all subjects for all conditions. Pearson correlation analysis was used since one of the two variables in each analysis was found to be normally distributed. Four outliers that were found in the data have been omitted. It is evident that there exist a significant, positive and good relationship between PSC and NOV for PCG ($N = 24$, Pearson's $r = 0.545$, $p < 0.05$). However, the relationship between PSC and NOV for SMA was found to be positive and significant but with fair association ($N = 24$, Pearson's $r = 0.442$, $p < 0.05$).

Dynamic causal modeling (DCM) analysis results

The results obtained from comparing Model 1 and Model 2 indicate that all subjects prefer PCG as the intrinsic input for UNI_{right} and UNI_{left} except for Subject 2 and Subject 7 who prefer SMA as the intrinsic input for UNI_{left}. Model 1 was then used in the second level in determining the intrinsic connectivity between PCG and SMA for UNI_{right} and UNI_{left} using two reduced models (Model 3 and Model 4) as shown in Figure 2. Model 3 has a uni-direction connection between PCG and SMA with PCG as the intrinsic input, while Model 4, which is Model 1 in the first level, has the input in PCG to be bi-directionally connected to SMA. Here, AIC and BIC criterion were again used in determining the most probable model. The input was later found to be bi-directionally connected to SMA.

The intrinsic connectivity model that has been determined for UNI is used to investigate the intrinsic connectivity within and between hemispheres during BIM in the third level. Taking PCG and SMA in both hemispheres as ROIs, five most probable models are constructed with the left and right PCGs as the intrinsic input, as shown in Figure 2. For Model 5 (or named as B1 in the third level analyses), any one ROI is in full connection (forward and backward) with other ROIs within and between hemispheres. Model B2 – Model B5 in Figure 2 are reduced models with limited connectivity between ROIs. These models are constructed based on orthodox assumption for motor activation in the cerebral cortices. The results of model comparison conducted on all models for all subjects are depicted in Fig. 6 and will be discussed in the following section.

DISCUSSION

Individual subject activation

The activation patterns obtained from individual subject are not perfectly the same in terms of activation area and intensity, as can be seen in Figure 3(a – d) for four out of seven subjects. For example, not all subjects activate a particular brain region and any subject may experience activation in many different areas and with different activation intensities. The differences between the results obtained from individual analysis on all subjects clearly show the subject-specific effects which are not always the same from subject-to-subject due to the intrinsic variability in each particular subject. These could be due to the differences in the BOLD signal intensity that is captured from each subject and may also arise due to subjects' different brain sensitivity when the task is performed, since the vasodilatory signal, cerebral blood flow (CBF), cerebral blood volume (CBV) and the quantity of deoxyhemoglobin which govern the height and spatial extent of the activation in the brain differ significantly in all individuals. The variability is thought to be intrinsic in nature since precautions in reducing the effects from confounding factors have been taken into consideration so as to assure that the fMRI experiment performed on all subjects is as similar as possible. Another possible source of variability is the inconsistency of the force and pace used by the subjects to tap their fingers, despite the training and tutorial given to the subjects prior to the fMRI scans. Previous studies[29,30] indicate that brain activation in cerebral motor cortices does depend on tapping frequency as well as tapping force. However, since the objective of this study was mainly focused on self-paced type of movement, slight differences in tapping force and frequency between subjects are expected to occur and will be taken into consideration in the interpretation of results. The fact that subjects' movements are not contributing to the observed activation is acceptable since those movement related effects, in particular the translational (x, y and z) as well as rotational (pitch, roll and yaw) motions have been excluded in generating the contrast images.

Group results

In our previous report on single subject[9], the inferences made on the subject are only valid for that particular subject and have a variance given by[31]

$$\sigma_w^2/n \qquad (1)$$

which is equivalent to the term $\mathrm{var}[{}_c^T\beta]$ as mentioned in[21] where n is the number of measurements for each subject and the subscript w denote within-subject variances. These inferences, however, are not valid for representing the whole group of subjects. For a multiple subject study, one can always make a statistical inference on a group of subjects by combining all the data obtained from the subjects by means of fixed effects analysis (FFX) or random-effects analysis (RFX)[32].

FFX considers the 840-volume acquisitions for all subjects as independent observations while ignoring serial correlation between acquisitions when making inference. In short, the error variance in FFX is estimated on scan-to-scan basis. The inference in RFX on the other hand is made by considering the variability in activation effects by assessing it from subject to subject. In another words, in the FFX, the samples are the combination of the scan volume (images) for all subjects whereas for the RFX, the number of sample is the number of contrast images of all subjects in this study, which is 7. Figure 4(a), which shows the results obtained from FFX, represents the average effects in the group from which the variance is said to originate from within-subject measurements only. The analyses involved all the seven subjects with a number of 840 measurements or scans; 420 scans during resting state, 140 scans during UNI_{right}, 140 scans during UNI_{left} and 140 scans during BIM (as compared to 60 scans during rest, 20 scans during UNI_{right}, 20 scans during UNI_{left} and 20 scans during BIM in the analysis done on single subject), with the assumption that each scan represents an independent observation with no serial correlation. The variance for the FFX can now be written as[33]

$$\sigma_w^2/Nn \qquad (2)$$

with N is the number of subject in the group and n is the number of measurement done on each subject. The error variance in FFX is also estimated on scan-to-scan basis but the degree of freedom in FFX is therefore the number of scans which is 840, minus the rank of the design matrix. Comparing Eqns. (1) and (2) implies that the effect size is larger and the variance is smaller for multiple subject FFX than that of the individual analysis resulting in a larger t value that is assigned to each voxel which is truly activated by the finger tapping task in this study. If the same height threshold is used in producing the SPMs, the resulting statistical images will have more activated voxels with higher signal intensities. With this method, FFX is able to exclude false positive voxels that are activated during individual analysis in which, failure to do so would lead to Type I error.

The statistical images in Figure 4(a) can be said to be the average statistical images for the seven subjects or, that the mean group response shows an activation. However, this does not constitute an inference that the group's responses is significant for every subject, for example, all subjects shows a consistent height and spatial activation characteristics. In other words, the FFX analysis is not suitable for making inferences about population effects but is perfectly valid for making inferences about the particular group of subjects studied. In order to make an inference that the population from which the subjects are drawn showed a significant activation, one would have to assess the variability in activation effects from subject to subject[15,33], for example in the random effects analysis (RFX).

The results depicted in Figures 4(b) are those obtained from RFX analysis. The appropriate error variance in RFX is based on the activation from subject to subject where the effect for each subject constitutes an independent observation and the degree of freedom is simply the number of subjects minus 1 (N - 1)[15]. As compared to the average effects of the group obtained from FFX, fewer voxels seem to be significantly active with lower intensity. This is because RFX analysis takes into account the between-subject variability which is normaly larger than that of between scans, resulting in a smaller t values. The population variance for RFX can be written as

$$\sigma_b^2/N + \sigma_w^2/Nn \qquad (3)$$

with the subscript b and w denote between-subject and within subject variances. The mean activation when compared to the variability in activation from subject to subject is smaller in terms of number of voxels and intensity due to the contribution from both the within-subject and between-subject variances in RFX. This concludes that the variability between subjects taken into consideration in the RFX is larger than the variability within subject for FFX[33]. A relatively smaller activation area with a reduction in signal intensity might also mean that the number of subjects are not enough for a valid statistical conclusion to be made upon a population. RFX is usually more conservative as compared to FFX. This method reflects the fact that the inference made can be generalised to the population from which the subjects were selected, given a proper number of subjects.The following discussions will be based on results generated by SPM by means of FFX and RFX on all subjects.

The corrected p values shown in Tables (2 – 4) are derived based on the set-level inferences (number of activated regions), cluster-level inferences (number of activated voxels) and voxel-level inferences (the p value for each voxel within the cluster[34]. The set-level inferences refer to the inferences that the number of clusters or set of clusters comprising an observed activation profile is highly unlikely to have occurred by chance. This level of inference is based on the probability of getting the observed number of clusters or more in the volume analysed, defined by a height and an spatial extent threshold.

The cluster-level inferences are a special case of set-level inferences that occur when the number of clusters are assumed to be equivalent to 1[34]. Defined by a height threshold, this procedure permit statistical inference to be made about each cluster and is based on the probability of getting a cluster of the size observed or a larger one in the volume

analysed. All the number of activated voxels in the clusters determined from the SPMs for all conditions are significant with $p_{FWE} < 0.05$. Similarly, voxel-level inferences are a special case of cluster-level inferences that result when the cluster is small. It is based on the probability that the observed voxel value or a higher one could have occurred by chance in the volume analysed. In Figures 4(a) and 4(b), only voxels that have a significant difference in intensity between active and rest are therefore shaded. Voxel-level tests permit individual vowels to be identified as significant, whereas cluster- and set-level inferences only allow clusters or set of clusters to be declared significant[34].

The typicality of the effects of the right, left and bimanual tapping of fingers in all subjects can be investigated using conjunction analyses. Conjunction analyses[15] provide a way to locate common features of functional anatomy between subjects under the same experimental condition. It expresses the typicality of the effects regardless of the presence of the effects in every subject. The results obtained from conjunction analysis simply demonstrate evidences that BA6, BA4a, BA4p and SMA are involved in motor processing for self-paced tapping of hand fingers in all subjects, as expected. Furthermore, it also concluded that the probability of this, occuring by chance, in the same area in each subject is still small which is denoted by the *p* value of a voxel obtained from the analyses.

Activation in the regions of interest (ROIs): spatial and height extent

Table 5(a) indicates that NOV decreases markedly as the level of significance increases. The 0 value of NOV denotes that not a single voxel survive the height threshold set by the α value. The results show that the corrected significance level placed a more stringent constraint in controlling the false positive activation. PCG seems to have a higher NOV as compared to SMA either in UNI or BIM types of finger tapping. This happens in all subjects at all significance levels. The behavior is supported by the average results obtained from group FFX and RFX. The group FFX and RFX results also show that the left hemisphere PCG and SMA (due to UNI_{right}) has a higher NOV as compared to the right hemisphere PCG and SMA (due to UNI_{left}), except for the RFX result at $\alpha < 0.001$ and $\alpha_{FWE} < 0.05$. For BIM, a similar results can be observed which shows a higher number of NOV in the left PCG and SMA except for FFX results at $\alpha = 0.1$ and RFX results at $\alpha = 0.001$ which indicate anomaly. On average, it can be concluded that during the UNI and BIM tapping of fingers, the PCG and SMA in the left hemisphere are more spatially activated as compared to their counterparts in the right hemisphere.

PSC is defined as the relative signal change within a cytoarchitectonic area evoked by the different experimental conditions, which reflects the involvement of that particular area in a specific task[25]. It is simply the ratio between the condition-specific signal change and the mean signal during the session. In this study, PSC for the PCG and SMA is calculated for a region of interest (ROI) of 4-mm radius, centered at the coordinates of the point of maximum intensity shown in Table 5(b). It is evident that the average PSC values obtained via FFX for PCG is always higher than for SMA for all conditions and are consistent in all subjects except for Subject 7 which indicates anomaly for UNI_{left} and BIM_{right} and Subject 1 for BIM_{left}. The average PSC values calculated from SPMs of FFX for PCG in the right hemisphere is always higher than in the left hemisphere for both UNI and BIM types of movement. However, the results for SMA is reversed where the left SMA shows higher PSC than the right for UNI and BIM types of finger tapping.

In our previous study on a single right-handed male subject[9], we found that the activated motor areas in the right hemisphere due to UNI_{left} showed a higher signal intensity and larger activation area as compared to that in the left hemisphere due to UNI_{right}. The results are similar for BIM in which the activation was observed in both hemispheres with the right hemisphere showing higher signal intensity and activation area. These findings are in good agreement with a previous multiple subject fMRI study[29] on unimanual and bimanual sequential movement in right-handers. They concluded that faster movement rates will cause higher activation both in terms of signal intensity and number of activated voxel, the so called "rate effects". They also found that the right hemisphere showed more activation than the left hemisphere both in UNI and BIM task at two tapping frequencies. Their interpretations are that right-handers expend more effort to perform with their non-preferred hand. A stronger activation pattern in the right hemisphere is the result of trying to perform with a system that is slightly less competent with the implication that the more skilled and competent system will expend less effort and will therefore provide a weaker activation[29]. As for the rate effects, they concluded that faster movement involves the recruitment of more motor units and will therefore activate a greater number of voxels[29]. Their findings are later reconfirmed in[35].

However, in the present study on multiple right-handed female subjects, the average responses over seven subjects obtained from FFX and RFX indicate higher height (signal intensity) and spatial (activation area) extent of activation in the left hemisphere for both UNI and BIM types of finger tapping as depicted in Figure 4(a) and (b) and Table 2 and 3. Furthermore, the FFX and RFX results on spatial extent of activation obtained from ROI analyses as tabulated in Table 5(a) also show similar findings from which it can be said that the total number of activated voxel in PCG (in which M1 is located) summed from all significant levels are roughly higher in the left hemisphere as compared to the right hemisphere. As mentioned earlier, this study used a self-paced finger tapping. Prior to the fMRI scan, the subjects were told that they need to tap their fingers two times in one second (using an intermediate force between too soft and

too hard). The subjects were also told to press all four fingers against the thumb beginning with the thumb-index finger contact and proceeding to the other fingers in sequence which would then begin anew with contact between thumb and index finger. However, since all the subjects are right-hand dominant, there will be a tendency for the subjects to tap their preferred hand fingers faster than their non-preferred hand fingers during UNI and BIM, resulting in the rate effects. Based on the interpretation given previously, it seemed that the influence of the rate effects is greater than the effects that would be produced by the average effects of the dominant and sub-dominant hand, hence producing greater activation in the left hemisphere. Interestingly, in contrast to the spatial extent of activation, the PSC for PCG obtained from ROI analyses of FFX data is higher in the right hemisphere (due to UNI_{left} and BIM_{left}) as compared to the PSC measured in the left hemisphere (due to UNI_{right} and BIM_{right}), see Table 5(b). In relation to the discussion above, it can be assumed that tapping rate does not influence the height extent of activation as it does on the spatial extent of activation. As a result, the higher PSC observed in the right hemisphere is due only to a higher control demand used by the brain in coordinating the tapping of the sub-dominant hand fingers.

The above results and discussion conclude on functional specialisation of human brain in performing motor task i.e. self-paced tapping of hand fingers. It is evident that BA1, BA4 (4a and 4p) and BA6 are consistently involved in all subjects in the execution of motor function in this study. These areas cover the precentral gyrus, postcentral gyrus, middle and superior frontal gyrus as well as the supplementary motor area. From group analyses on multiple subjects, it is quite interesting to see that the left side of the brain (triggered by the tapping of the right hand fingers) shows a larger number of activated voxel and higher activation intensity as compared to the right side of the brain (triggered by the left-hand finger tapping), as opposed to our previous study on a single male subject, despite the fact that all the subjects are right handed. This shows the reliability of multiple subjects analyses in making inferences over a population. Moreover, group results indicate the existence of ipsilaterality accompanying the expected contralaterality, which in turn raises the question of connectivity. The latter will partly be answered in our following analyses on the dynamic behavior of the human brain using the ROI and DCM approaches. The analyses is focused on two anatomical regions that are known to be involved in controlling motor movement which are the primary motor cortex which is composed of BA4 of the precentral gyrus (will be named as PCG) and SMA which located in the medial part of BA6. SMA is also known to be involved in planning complex movements and in coordinating movements involving both hands.

Effective connectivity

Based on the results shown in Table 6, for UNI_{right}, all subjects are in favour of Model 4. However, for UNI_{left}, four (Subject 1, 2, 3 and 7) out of seven subjects prefer a uni-direction connection from PCG to SMA, which is represented by model 3. The intrinsic input of PCG and the connectivity between PCG and SMA for all subjects together with their posterior probability are tabulated in Table 6. It can be clearly seen that for UNI_{right}, all the inputs and the connections PCG→SMA and SMA→PCG have posterior probability of greater than 0.9, which means that there is a 90% probability of the connection to occur. According to[13], an effective connectivity between any two ROIs can be accepted if its value is relatively high with a posterior probability greater than 0.9. For UNI_{left}, Subject 1, 2, 3 and 7 shows the posterior probability of less than 0.9 for SMA→PCG connection while PCG→SMA connection has the probability value of less than 0.9 only for subject 1, but the respective connectivity values are relatively large. If a lower cut-off value for intrinsic probability is considered i.e. 0.8, most subjects will have a preference to Model 4. To conclude on the effective connectivity between the two respective ROIs for UNI in both hemispheres, it can be said that Model 4 is the most probable model that can represent the transmission of signal between PCG and SMA during the unimanual tapping of right and left hand fingers, with PCG as the intrinsic input.

The results from DCM analyses have interestingly shown the occurrence of inter-hemispheric connection between PCG_{right} and PCG_{left} that mediate motor coordination during BIM. The full connectivity model as shown by Model B1 is not a preference. So do models that have inter-hemispheric connections such as $SMA_{right} \leftrightarrow SMA_{left}$, $SMA_{right/left} \leftrightarrow PCG_{left/right}$. However, $PCG_{right/left} \leftrightarrow PCG_{left/right}$ connections do exist in all subjects with the exception of Subject 2 and 5. From the results of the Bayesian model selection (BMS) depicted in Figure 6 for all subjects, it can be concluded that all subjects are in favor of Model B3 with the exception of Subject 1 from which it can be observed that AIC and BIC are in good agreement on Model B3 for most of the subject. The strength of the intrinsic input and connectivity and their posterior probabilities obtained from DCM analyses on Model B3 for all subjects are tabulated in Table 7. All the intrinsic inputs through PCG have values of posterior probability larger than 0.9. It can also be seen that the effective connectivity between PCG→SMA is relatively large with the posterior probability of 1.0000 for most connections. However, most of the subjects show SMA→PCG connection that has the posterior probability values of less than 0.9 which indicate a uni-direction nature of PCG-SMA connection during bimanual tapping of hand fingers.

A comprehensive study has been done by Grefkes *et al.*[11] to investigate the dynamic intra- and interhemispheric interactions during unilateral and bilateral hand movements using fMRI and DCM. The aim was to estimate connectivity among key areas of the motor system, namely PCG, SMA and PMC. However, the study used full hand movements

Table 6 The values of the intrinsic input at precentral gyrus (PCG) and intrinsic connectivity between PCG and supplementary motor area (SMA) and SMA and PCG based on Model 4 for unimanual (UNI_{right} and UNI_{left}). The intrinsic connectivity which has the posterior probability (shown in parenthesis) of less than 0.9 is given in italic

Subject	UNI_{right} (Left Hemisphere)			UNI_{left} (Right Hemisphere)		
	Intrinsic input (PCG)	PCG to SMA	SMA to PCG	Intrinsic input (PCG)	PCG to SMA	SMA to PCG
1	0.0870 (1.0000)	0.8782 (1.0000)	0.8250 (1.0000)	0.1779 (0.9884)	*0.2662 (0.8462)*	*0.1110 (0.6157)*
2	0.1372 (0.9998)	0.7754 (1.0000)	0.7321 (0.9996)	0.2962 (0.9991)	0.4448 (0.9992)	*0.3796 (0.8653)*
3	0.2358 (1.0000)	0.5923 (1.0000)	0.8299 (0.9996)	0.2299 (0.9945)	0.3932 (0.9457)	*0.0161 (0.5172)*
4	0.1701 (1.0000)	0.7482 (1.0000)	0.8442 (1.0000)	0.1902 (0.9997)	0.5719 (0.9999)	0.7276 (0.9951)
5	0.1574 (0.9997)	0.5504 (0.9999)	0.9346 (0.9995)	0.2399 (1.0000)	0.3684 (0.9997)	0.8131 (0.9942)
6	0.4189 (1.0000)	0.4285 (1.0000)	0.9782 (0.9996)	0.3910 (1.0000)	0.4668 (1.0000)	1.2313 (1.0000)
7	0.1482 (1.0000)	0.7774 (1.0000)	0.9831 (1.0000)	0.3884 (0.9945)	0.7576 (0.9996)	0.2497 *(0.8019)*

Table 7 The values of the intrinsic input at the right precentral gyrus (PCG_{right}) and left precentral gyrus (PCG_{left}) and the intrinsic connectivity between precentral gyrus (PCG) and supplementary motor area (SMA) in and between hemispheres based on Model B3 for bimanual (BIM). The intrinsic connectivity which has the posterior probability (shown in parenthesis) of less than 0.9 is given in italic

Subject	BIM_{right} (Left Hemisphere)			BIM_{left} (Right Hemisphere)			Inter Hemisphere	
	Intrinsic input (PCG)	PCG to SMA	SMA to PCG	Intrinsic input (PCG)	PCG to SMA	SMA to PCG	PCG_{right} to PCG_{left}	PCG_{left} to PCG_{right}
1	0.8616 (1.0000)	0.2056 (1.0000)	*0.1243 (0.7351)*	0.1861 (0.9152)	0.3131 (1.0000)	*0.0956 (0.6872)*	0.2631 (0.9223)	0.3319 (0.9883)
2	0.1979 (0.9916)	0.2874 (0.9762)	*0.0632 (0.6239)*	0.1620 (0.9938)	0.4220 (0.9983)	*0.1358 (0.7552)*	*0.1366 (0.7571)*	*0.1913 (0.8403)*
3	0.1468 (0.9888)	0.2737 (0.9800)	*0.1452 (0.7688)*	0.1711 (0.9970)	0.2967 (0.9966)	*0.1862 (0.8288)*	0.4068 (0.9906)	0.4176 (0.9914)
4	0.2720 (0.9997)	0.3429 (0.9999)	*0.0946 (0.6864)*	0.2175 (0.9990)	0.5404 (1.0000)	0.2374 (0.9056)	0.2394 (0.9194)	0.3074 (0.9573)
5	0.1097 (0.9682)	0.4102 (0.9996)	*0.1745 (0.8177)*	0.2440 (0.9996)	0.2907 (0.9978)	*0.0803 (0.6578)*	0.3588 (0.9779)	*0.1828 (0.8390)*
6	0.8616 (1.0000)	0.2056 (1.0000)	*0.1243 (0.7351)*	0.1861 (0.9152)	0.3131 (1.0000)	*0.0956 (0.6872)*	0.2631 (0.9223)	0.3319 (0.9883)
7	0.1835 (0.9847)	0.3701 (1.0000)	0.3341 (0.9594)	0.1176 (0.9835)	0.5567 (1.0000)	0.3385 (0.9678)	0.7023 (1.0000)	0.5469 (0.9999)

rather than isometric finger tapping. They also used video screen to inform the subjects on which hand to move (right, left or bimanual). In their DCM analyses, they used complex models with modulatory inputs in addition to the intrinsic inputs and intrinsic couplings to model the influence of one area on the coupling of interactions between the other two areas. They found an intrinsic balance of excitatory and inhibitory couplings among core regions within and across hemispheres. Another important finding is that SMA has been found to be the key structure promoting or suppressing activity in the cortical motor network during unimanual and bimanual hand movements.

The results of the present study cannot be compared with that of Grefkes *et al*.[11] since this study concentrated only on two motor areas which are M1 (in PCG) and SMA, excluding PMC. Furthermore, due to the experimental limitations, we did not include modulatory inputs in the model to be estimated by DCM since no video screen was used to instruct the subject on the task that they should commence so that there will be at least one area in the brain that will act as modulatory input. However, despite the limitations, some of the results on the effective connectivity that have been obtained are quite similar with that of Grefkes *et al*.[11], for example the existence of $PCG_{right} \leftrightarrow PCG_{left}$ bilateral connections, the role of SMA in coordinating the unimanual and bimanual types of movement and the role of M1 as the input centre. An extension to the present study is necessary in order to investigate the applicability of more complex models on the present data as suggested by Grefkes *et al*.[11].

CONCLUSION

The results of FFX obtained from this multiple-subject study on right-handed female subjects showed that the observed brain activation for UNI_{right} and UNI_{left} fulfill contralaterality behavior of motor coordination with a larger activation area for UNI_{right}. The activation for BIM however occurs in both hemispheres with BIM_{right} showing a higher activation intensity and area as compared to BIM_{left}. Analyses performed on the same data sets using random-effects analysis (RFX) yield similar results. Conjunction analysis indicates the primary motor area (M1) in the precentral gyrus (PCG) as the common activated area for all conditions in all subjects.

ROI analyses for FFX and RFX reveal that the number of activated voxel (NOV) and percentage of signal change (PSC) on average is higher in PCG than SMA for all tapping conditions. However, comparing between hemispheres for both UNI and BIM, higher PSC is observed in the right PCG and the left SMA. There exist some sort of positive association between PSC and NOV of the ROIs which needs further investigations.

DCM model selection results indicate that all subjects prefer PCG as the intrinsic input for UNI_{right} and UNI_{left} except for Subject 2 and Subject 7 who prefer SMA as the intrinsic input for UNI_{left}. The input was later found to be bi-directionally connected to SMA for UNI_{right}. However, for UNI_{left}, four out of seven subjects prefer a uni-direction connection from PCG to SMA. The bi-directional model was then used for BIM in the left and right hemispheres. The model was in favour of six out of seven subjects. DCM analyses concluded that during selp-paced finger tapping, there exists only one interhemispheric connectivity which is between PCG_{right} and PCG_{left}. The findings are strong evidence of the existence of functional specialisation and integration i.e. effective connectivity in human brain during finger tapping and can be used as baselines in determining the probable motor coordination pathways and their connection strength in normal subjects. Finally, it is worth to mention that the statistical parametric mapping (SPM), by means of the fixed and random-effects analyses has proven to be a suitable tool in the analysis of functional imaging data obtained from an fMRI experiment which includes the study of functional specialisation of human brain, the percentage of signal change and the effective connectivity that occurs between several activated regions in the brain.

ACKNOWLEDGEMENT

The authors would like to thank Sa'don Samian, the MRI Technologist of Universiti Kebangsaan Malaysia Hospital (HUKM), for his assistance in scanning and the Department of Radiology, Universiti Kebangsaan Malaysia Hospital for the permission to use the MRI scanner. The authors were also indebted to Professor Karl J. Friston and the functional imaging group of the University College of London for valuable discussions on experimental methods and data analyses. This work is supported by the research grants IRPA 09-02-02-0119EA296, the Ministry of Science, Technology and Innovation of Malaysia and and UKM-GUP-SK-07-20-205, Universiti Kebangsaan Malaysia.

REFERENCES

[1] Friston KJ. Models of brain function in neuroimaging. Annu Rev Psychol 2005; 56: 57-87.

[2] Turner R. Functional mapping of the human brain with magnetic resonance imaging. The Neuroscience 1995; 7: 179-194.

[3] Amaro EJ, Barker GJ. Study design in fMRI : Basic principles. Brain and Cognition 2006; 60: 220-232.

[4] Mansfield P. Multiplanar image formation using NMR spin echoes. J Phys C 1977; 10: L55-L58.

[5] Bernstein MA, King KF, Zhou XJ. Handbook of MRI pulse sequences. Burlington: Elsevier Academic Press, 2004.

[6] Ogawa S, Lee TM, Nayak AS, Glynn P. Oxygenation-sensitive contrast in magnetic resonance imaging of rodent brain at high magnetic fields. Magn Reson Med 1990; 14: 68-78.

[7] Ogawa S, Lee TM. Magnetic resonance imaging of blood vessels at high fields: in vivo and in vitro measurements and image simulation. Magn Reson Med 1990; 16: 9-18.

[8] Ogawa S, Lee TM, Kay AR, Tank DW. Brain magnetic resonance imaging with contrast dependent on blood oxygenation. Proc Natl Acad Sci USA 1990; 87: 9868-9872.

[9] Ahmad Nazlim Yusoff, Mohd Harith Hashim, Mohd Mahadir Ayob, Iskandar Kassim, Nur Hartini Mohd Taib and Wan Ahmad Kamil Wan Abdullah. Functional specialization and connectivity in cerebral motor cortices: A single subject study using fMRI and statistical parametric mapping. Mal J Med Health Sci 2006; 2(2): 37-60.

[10] Toga AW, Thompson PM. An introduction to maps and atlases of the brain. In : A. W. Toga and J. C. Mazziotta (Eds.), Brain Mapping : The Systems, San Diego, U.S.A. : Academic Press 2000; 3-32.

[11] Grefkes C, Eickhoff SB, Nowak DA, Dafotakis M, Fink GR. Dynamic intra- and interhemispheric interactions during unilateral and bilateral hand movements assessed with fMRI and DCM. Neuroimage 2008; 41: 1382-1394.

[12] Penny WD, Stephan KE, Mechelli A, Friston KJ. Comparing dynamic causal model. Neuroimage 2004; 22: 1157-1172.

[13] Friston KJ, Harrison L, Penny W. Dynamic causal modeling. Neuroimage 2003; 19: 1273-1302.

[14] Desmond JE, Glover, GH. Estimating sample size in functional MRI (fMRI) neuroimaging studies: Statistical power analysis. J Neurosci Methods 2002; 118: 115-128.

[15] Friston KJ. Experimental design and statistical parametric mapping. In: Frackowiak RSJ, Friston KJ, Frith CD, Dolan RJ, Price CJ, Zeki S, Ashburner J and Penny WD (Eds.). Human Brain Function. Amsterdam : Elsevier Academic Press 2004: 599-632.

[16. Ashburner J, Good CD. Spatial registration of images. In: Tofts P (Ed.), Quantitative MRI of the Brain: Measuring Changes Caused by Disease. West Sussex, England: John Wiley & Sons Ltd 2003: 503-531.

[17] Ashburner J, Friston KJ. Computational Neuroanatomy. In: Frackowiak RSJ, Friston KJ, Frith CD, Dolan RJ, Price CJ, Zeki S, Ashburner J, Penny WD (Eds.), Human Brain Function. Amsterdam : Elsevier Academic Press 2004: 655-672.

[18] Ahmad Nazlim Yusoff, Mohd Harith Hashim, Mohd Mahadir Ayob, Iskandar Kassim. Pengimejan resonans magnet kefungsian: Pemerolehan, analisis dan pentafsiran data. J Sains Kes Mal 2005; 3(2): 19-37.

[19] Ahmad Nazlim Yusoff, Mohd Harith Hashim, Mohd Mahadir Ayob, Iskandar Kassim. Analisis data pengimejan resonans magnet kefungsian: Pra pemprosesan ruang menggunakan kaedah pemetaan statistik berparameter. J Sains Kes Mal 2006; 4(1): 21-36.

[20] Ahmad Nazlim Yusoff, Mohd Harith Hashim, Mohd Mahadir Ayob, Iskandar Kassim. Pengaktifan otak akibat gerakan jari bagi subjek dominan tangan kanan dan kiri. J Sains Kes Mal 2006; 4(2): 63-83.

[21] Ahmad Nazlim Yusoff, Mazlyfarina Mohamad, Mohd Mahadir Ayob, Mohd Harith Hashim. Brain activations evoked by passive and active listening: A Preliminary Study On Multiple Subjects. J Sains Kes Mal 2008; 6(1): 35-60.

[22] Tzourio-Mazoyer N, Landeau B, Papathanassiou D, Crivello F, Etard O, Delcronix N, *et al*. Automated anatomical

labeling of activations in SPM using a macroscopic anatomical parcellation of the MNI MRI single-subject brain. Neuroimage 2002; 15: 273-289.

[23] Maldijan JA, Laurienti PJ, Kraft RA, Burdette JH. An automated method for neuroanatomic and cytoarchitectonic atlas-based interrogation of fMRI data sets. Neuroimage 2003; 19(3): 1233-1239.

[24] Worsley K, Marrett S, Neelin P, Vandal A, Friston K, Evans A. A unified statistical approach for determining significant signals in images of cerebral activation. Human Brain Mapping 1996; 4: 58-73.

[25] Matthew Brett, Jean-Luc Anton, Romain Valabregue, Jean-Baptiste Poline. Region of interest analysis using an SPM toolbox. Proceedings of the 8th International Conference on Functional Mapping of the Human Brain; 2002 June 2–6: Sendai Japan. Available in CD-ROM in Neuroimage 2002; 16(2).

[26] Eickhoff SB, Stephan KE, Mohlberg H, Grefkes C, Fink GR, Amunts K et al. A new SPM toolbox for combining probabilistic cytoarchitectonic maps and functional imaging data. NeuroImage 2005; 25: 1325-1335.

[27] Talairach J, Tournoux P. Coplanar stereotaxic atlas of the human brain. New York: Thieme Medical, 1988.

[28] Collins DL, Neelin P, Peters TM, Evans AC. Automatic 3D intersubject registration of MR volumetric data in standardized Talairach space. J. Compute. Assist. Tomogr 1994; 18: 192-205.

[29] Jäncke L, Peters M, Schlaug G, Posse S, Steinmetz H, Müller-Gartner, H-W. Differential magnetic resonance signal change in human sensorimotor cortex to finger movements of different rate of the dominant and subdominant hand. Cogn Brain Res 1998; 6: 279-284.

[30] Wildgruber D, Erb M, Klose U, Grodd W. Sequential activation of supplementary motor area and primary motor cortex during self-paced finger movement in human evaluated by functional MRI. Neurosci. Lett 1997; 227: 161-164.

[31] Penny W, Holmes AJ. Random-effects analysis. In: Frackowiak RSJ, Friston KJ, Frith CD, Dolan RJ, Price CJ, Zeki S, Ashburner J and Penny WD (Eds.). Human Brain Function. Amsterdam : Elsevier Academic Press 2004: 843-849.

[32] Snijders TAB. Fixed and random effects. In: Everitt BS, Howell DC (Eds), Encyclopedia of Statistics in Behavioural Science, Vol. (2), Chicester: Wiley 2005: 664-665.

[33] Penny W. Introduction to random field theory. In: Frackowiak RSJ, Friston KJ, Frith CD, Dolan RJ, Price CJ, Zeki S, Ashburner J and Penny WD (Eds.). Human Brain Function. Amsterdam : Elsevier Academic Press 2004: 867-879.

[34] Friston KJ, Holmes A, Poline JB, Price CJ, Frith CD. Detecting activations in PET and fMRI: Levels of inference and power. NeuroImage 1996; 40: 223-235.

[35] Lutz K, Koeneke S, Wustenberg T, Jäncke L. Asymmetry of cortical activation during maximum and convenient tapping speed. Neurosci. Lett 2005; 373: 61-66.